

Observation of the period ratio P_1/P_2 of transversal oscillations in solar macro-spicules

H. Ebadi, and M. Khoshrangbaf

Abstract We analyze the time series of oxygen line profiles (OVI 1031.93 Å and OVI 1037.61 Å) obtained from SUMER/SOHO on the solar south limb. We calculated Doppler shifts and consequently Doppler velocities in three heights 4'', 14'', and 24'' from the limb on a coronal hole region. Then, we performed wavelet analysis with Morlet wavelet transform to determine the periods of fundamental mode and its first harmonic mode. The calculated period ratios have departures from its canonical value of 2. The density stratification and magnetic twist are two main factors which may cause these departures.

Keywords Sun: spicules · MHD waves: period ratio

1 Introduction

Observation of oscillations in solar spicules may be used as an indirect evidence of energy transport from the photosphere towards the corona. Transverse motion of spicule axis can be observed by both, spectroscopic and imaging observations. The periodic Doppler shift of spectral lines have been observed from ground based coronagraphs (Nikolsky & Sazanov 1987; Kukhianidze et al. 2006; Zaqarashvili et al. 2007). But Doppler shift oscillations with period of ~ 5 min also have been observed on the SOlar and Heliospheric Observatory (*SOHO*) by Xia et al. (2005). Direct periodic displacement of spicule axes have been found by imaging observations on Solar Optical Telescope (SOT) on *Hinode* (De Pontieu et al. 2007; Kim et al. 2008; He et al. 2009).

The observed transverse oscillations of spicule axes were interpreted by kink (Nikolsky & Sazanov 1987; Kukhianidze et al. 2006; Zaqarashvili et al. 2007; Kim et al. 2008; Ebadi et al. 2012a) and Alfvén (De Pontieu et al. 2007) waves. All spicule oscillations events are summarized in a recent review by Zaqarashvili & Erdélyi (2009). They suggested that the observed oscillation periods can be formally divided in two groups: those with shorter periods (< 2 min) and those with longer periods (≥ 2 min) (Zaqarashvili & Erdélyi 2009). The most frequently observed oscillations lie in the period ranges of 3–7 min and 50–110 s. Additionally, very long spicules, called as macrospicules by Bochlin et al. (1975) with a typical length of up to 40 Mm are frequently observed mostly near the polar regions as reported by, e.g., Pike & Harrison (1997); Doyle et al. (2005); Scullion et al. (2009); Murawski et al. (2011).

One of the most important functions of coronal seismology is determining the period ratio P_1/P_2 between the period P_1 of the fundamental mode and the period P_2 of its first harmonic (Andries et al. 2009; Karami & Bahari 2012; Orza et al. 2012; Erdélyi et al. 2013). Different factors such as the effect of density stratification (Andries et al. 2009) and magnetic twist (Karami & Bahari 2009) can cause the deviation of the period ratio from its canonical value of 2. The observed values of this ratio in coronal loops is either smaller or larger than 2 (Verwichte et al. 2004; Andries et al. 2009). Srivastava et al. (2008) Using simultaneous high spatial and temporal resolution H α observations studied the oscillations in the relative intensity to explore the possibility of sausage oscillations in the chromospheric cool post-flare loop. They used the standard wavelet tool, and find $P_1/P_2 \sim 1.68$. They suggested that the oscillations represent the fundamental and the first harmonics of the fast-sausage waves in the cool post-flare loop. Verwichte et al. (2004) have detected interesting

H. Ebadi, and M. Khoshrangbaf

Astrophysics Department, Physics Faculty, University of Tabriz, Tabriz, Iran

e-mail: hosseinebadi@tabrizu.ac.ir

phenomenon of simultaneous existence of fundamental and first harmonics of fast-kink oscillations (see also De Moortel & Brady (2007); Van Doorselaere et al. (2007); Zaqarashvili et al. (2013a)). However, the ratio between the periods of fundamental and first harmonics P_1/P_2 was significantly shifted from 2, which later was explained as a result of longitudinal density stratification in the loop. The rate of the shift allows us to estimate the density scale height in coronal loops, which can be a few times larger compared to its hydrostatic value.

Observed oscillation periods can be used to estimate the Alfvén speed and consequently magnetic field strength in macro-spicules (Zaqarashvili et al. 2013b).

The mentioned studies in the previous paragraph are all devoted to the coronal loop transversal oscillations. To my knowledge there is no any work related to the period ratio of spicules oscillations. So, the present study is an attempt to check this ratio observationally. We will study the same problem theoretically in our future works.

2 Observations and data processing

SUMER is a high-resolution normal incidence spectrograph operating in the range $666\text{--}1610\text{Å}$ (first order) and $333\text{--}805\text{Å}$ (second order). The angular pixel size is $\sim 1''$. The spectral pixel size depends slightly on the wavelength. Contriving normally allows sub-pixel resolution. It can vary from about 45 mÅ/pixel at 800Å to about 41 mÅ/pixel at 1600Å (Wilhelm et al. 1995).

A coronal hole region in the south pole of the sun was observed with SUMER (detector B) on 21 Feb 1997. The pointing coordinates were $X = 0''$, $Y = -985''$. The slit, which was used for observations, has the dimensions of $0.3'' \times 120''$. The observation was performed from 01:36 UT to 01:52 UT and the exposure time was 15 seconds. In Figure 1 we presented the images of the studied region which were observed by 304Å SOHO/EIT (top) on 21 February 1997. The rectangular shows the region of south limb macro-spicules. We used the “madmax” algorithm to enhance the finest structures (Koutchmy & Koutchmy 1989). As it is clear from down panel of Figure 1, the length of the studied spicule is 25 Mm which means that the studied spicule is macro-spicule. Since the EIT images have a fixed pixel resolution of 2.5 arcsec so, the down panel of Figure 1 is the best quality after image processing techniques.

The raw data have been initially processed applying the standard procedures for flatfield, deadtime and de-stretching correction which can be found in the Solar

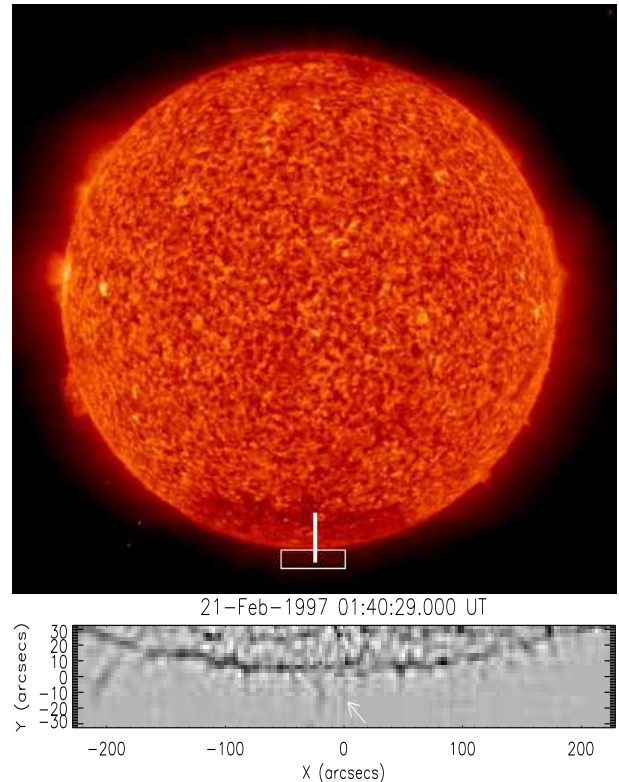


Fig. 1 Image of the studied region which were observed by 304Å SOHO/EIT (top) on 21 February 1997. The slit is in the North–South direction. The rectangular shows the region studied. We used the “madmax” algorithm to enhance the finest structures (down). The white arrow shows the studied macro-spicule.

Software (SSW) database. We performed the radiometric calibration, so the specific intensity unit is $\text{W m}^{-2} \text{sr}^{-1} \text{\AA}^{-1}$ through this analysis (Ebadi et al. 2007; Vial et al. 2009).

We calculated the integrated intensity for OVI (1031.93 \AA) line along the SUMER slit. The limb is located in pixel number 86 and the spicule region is lied from pixel 87 to 117 which is shown in Figure 2. Moreover, we plotted integrated profile of OVI (1031.93 \AA) line in Figure 3.

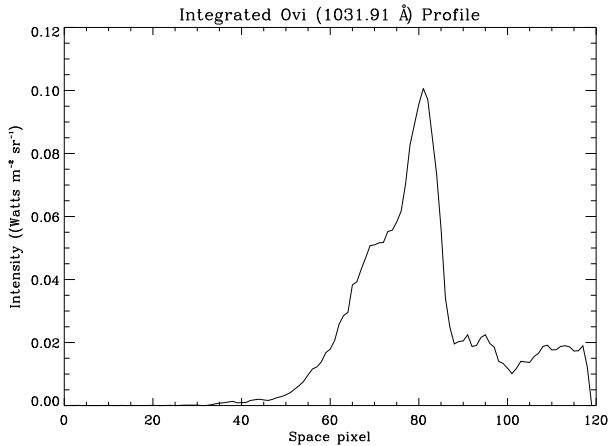


Fig. 2 The integrated intensity along the SUMER slit for OVI (1031.93 \AA) line. The spicule region is lied from pixel 87 to 117.

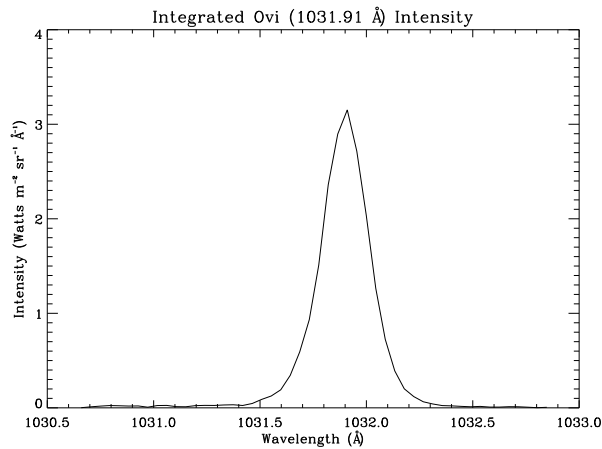


Fig. 3 The integrated profile of OVI (1031.93 \AA) line.

3 Results and Discussion

We analyze OVI (1031.93 \AA) and OVI (1037.61 \AA) line profiles from the time series by fitting to a Gaussian. Then we calculated Doppler shifts and consequently

Doppler velocities (Zaqarashvili et al. 2007). we used the two stable photospheric neutral oxygen emission lines (i.e. OI (1027.43 \AA) and OI (1028.16 \AA)) that happen to be in the same spectral window with the OVI lines. Doppler velocities and proper wavelet analysis results are presented in Figures 4, 5, and 6 for OVI (1031.93 \AA). We perform wavelet analysis with Morlet wavelet transform in three heights for both lines. On the other hand, wavelet analysis results for the line OVI (1037.61 \AA) are showed in Figures 7, 8, and 9. The wavelet power spectrum, the cone of influence, and the global wavelet power spectrum are plotted in each figure. The contour levels are chosen so that 75%, 50%, 25%, and 5% of the wavelet power is above each level, respectively.

We determined the fundamental mode and its first harmonic periods for each line and in three heights (4'', 14'', and 24'' from the limb). For comparison we presented results in Table 1 for both lines.

Table 1 P_1 (fundamental mode period), P_2 (first harmonic period), and P_1/P_2 (fundamental to its first harmonic period ratio) are presented for both oxygen lines.

line	height	P_1 (s)	P_2 (s)	P_1/P_2
OVI(1031.93 \AA)	4''	96	45	2.13
OVI(1031.93 \AA)	14''	100	48	2.08
OVI(1031.93 \AA)	24''	110	50	2.2
OVI(1037.61 \AA)	4''	108	52	2.07
OVI(1037.61 \AA)	14''	118	58	2.03
OVI(1037.61 \AA)	24''	100	49	2.04

As it is clear from the Table 1, the fundamental mode and its first harmonic period ratios have departures from its canonical value of 2. They are greater than 2 in both lines in 4'', 14'', and 24'' from the limb. The fundamental mode periods are determined as 96–118 s and its first harmonic periods are lied in the range 45–58 s. These periods are in good agreement with the results of previous works in this area (Kukhianidze et al. 2006; Ebadi et al. 2012a,b; Ebadi 2013). It should be noted that these periods and their ratios are related to a unique macro-spicule. It is shown in Figure 1 that the SUMER slit covers only one macro-spicule.

The density stratification and magnetic twist are two main factors which make the period ratio departures from its canonical value of 2. These two factors are studied in spicules both observationally and theoretically. The first estimation of spicule magnetic field by spicule seismology was done by Zaqarashvili et al. (2007). Verth et al. (2011) based on SOT/*Hinode* observations determined the variation of magnetic field

strength and plasma density along a spicule by seismology. They studied a kink wave propagating along a spicule by estimating the spatial change in phase speed and velocity amplitude as a novel approach. Suematsu et al. (2008); Tavabi et al. (2011) by using the SOT/*Hinode* observations reported twisted motions in spicules.

Since we determined the oscillation periods of fundamental mode and its first harmonic in macro-spicules, it is possible to estimate the Alfvén speed and consequently magnetic field strength through them. Kink waves are transverse oscillations of magnetic tubes and the phase speed for a straight homogenous tube can be written as:

$$c_k = \frac{\lambda}{T_{obs}} = V_{A0} \sqrt{\frac{2}{1 + \rho_e/\rho_0}}, \quad (1)$$

where $V_{A0} \equiv B_0/\sqrt{\mu_0\rho_0}$ is the Alfvén speed inside the tube, λ is the wavelength, and T_{obs} is the observed oscillation period. ρ_e and ρ_0 are the plasma density outside and inside of tube, respectively. The density in spicules is $3 \times 10^{-10} \text{ kg m}^{-3}$ and $\rho_e/\rho_0 \simeq 0.02$ (Zaqarashvili & Erdélyi 2009; Ebadi et al. 2012a). For the fundamental mode, $\lambda = 2L$ (L is the length of the macro-spicule which determined as 25 Mm in this work). The mean fundamental mode period is determined as ~ 105 s. By using these parameters in Equation 1 the Alfvén speed and magnetic field strength is estimated as $\sim 340 \text{ km/s}$ and $\sim 65 \text{ G}$ in macro-spicules, respectively.

4 conclusion

We analyze the time series of OVI (1031.93 Å) and OVI (1037.61 Å) line profiles obtained from SUMER/SOHO in order to uncover the oscillations in the solar macro-spicules. We concentrate on particular coronal hole region which contains the macro-spicules and found that their axis undergo quasi-periodic transverse displacement. This is done by calculating Doppler shifts and consequently Doppler velocities in three heights 4'', 14'', and 24'' from the limb. By performing wavelet analysis with Morlet wavelet transform in three heights we determine the fundamental mode and its first harmonic periods and their ratios. Our findings show small departures of this value from its canonical value of 2 in both lines and three mentioned heights. In other words, they are greater than 2 in both lines in 4'', 14'', and 24'' from the limb. These departures may be caused by the density stratification and magnetic twist which is observed in spicules. Observed oscillation periods

are used to estimate the Alfvén speed and consequently magnetic field strength in macro-spicules as $\sim 340 \text{ km/s}$ and $\sim 65 \text{ G}$, respectively.

Acknowledgements The authors thank anonymous referee for his/her useful and instructive comments in improving the document. The authors are grateful to the *SOHO* Team for providing the observational data. SUMER is financially supported by DLR, CNES, NASA and the ESA PRODEX program (Swiss contribution). SOHO is a mission of international cooperation between ESA and NASA. We appreciate the ISSI support in the frame of the "Spectroscopy and Imaging of coronal hole spicules from Space" Team.

References

- Andries, J., van Doorselaere, T., Roberts, B., Verth, G., Verwichte, E., Erdélyi, R.: *Space Sci. Rev.* **149**, 3 (2009)
- Bochlin, J.D., et al.: *Astrophys. J.* **197**, 133 (1975)
- De Moortel, I., Brady, C. S.: *Astrophys. J.* **664**, 1210 (2007)
- De Pontieu, B., McIntosh, S.W., Carlsson, M., et al.: *Science* **318**, 1574 (2007)
- Doyle, J. G., Giannikakis, J., Xia, L. D., Madjarska, M. S.: *Astron. Astrophys.* **431**, 17 (2005)
- Ebadi, H., Vial, J.-C., Ajabshirizadeh, A.: *Sol. Phys.* **257**, 91 (2007)
- Ebadi, H.: *Astrophys. Space Sci.* **348**, 11 (2013)
- Ebadi, H., Zaqarashvili, T.V., Zhelyazkov, I.: *Astrophys. Space Sci.* **337**, 33 (2012a)
- Ebadi, H., Zaqarashvili, T.V., Zhelyazkov, I.: *AIP Conference Proceedings*, **1356**, 117 (2012b)
- Erdélyi, R., Hague, A., Nelson, C. J.: *Sol. Phys.* Doi:10.1007/s11207-013-0344-2 (2012)
- He, J., Marcs, E., Tu, G., Tian, H.: *Astrophys. J. Lett.* **705**, L217 (2009)
- Karami, K., Bahari, K.: *Astrophys. J.* **757**, 186 (2012)
- Karami, K., Bahari, K.: *Mon. Not. R. Astron. Soc.* **394**, 521 (2009)
- Kim, Y.H., Bong, S.C., Park, Y.D., Cho, K.S., Moon, Y.J., Suematsu, Y.: *J. Korean Astron. Soc.* **41**, 173 (2008)
- Koutchmy, O., Koutchmy, S.: In: O. von der Lühe (ed.): *High Spatial Resolution Solar Observations: Proceedings of the Tenth Sacramento Peak Summer Workshop (Sunspot, NM, August 22–26, 1988)*, p. 217, National Solar Observatory/Sacramento Peak, Sunspot, NM 88349 (1989)
- Kukhianidze, V., Zaqarashvili, T.V., Khutsishvili, E.: *Astron. Astrophys.* **449**, 35 (2006)
- Murawski, K., Srivastava, A. K., Zaqarashvili, T. V.: *Astron. Astrophys.* **535**, 58 (2011)
- Nikolsky, G.M., Sazanov, A.A.: *Soviet Astron.* **10**, 744 (1967)
- Orza, B., Ballai, I., Jain, R., Murawski, K.: *Astron. Astrophys.* **537**, 41 (2012)
- Pike, C. D., Harrison, R. A.: *Sol. Phys.* **175**, 457 (1997)
- Scullion, E., Popescu, M. D., Banerjee, D., Doyle, J. G., Erdélyi, R.: *Astrophys. J.* **704**, 1385 (2009)

-
- Srivastava, A. K., Zaqarashvili, T. V., Uddin, W., Dwivedi, B. N., Kumar, Pankaj: *Mon. Not. R. Astron. Soc.* **388**, 1899 (2008)
- Suematsu, Y., Ichimoto, K., Katsukawa, Y., Shimizu, T., Okamoto, T., Tsuneta, S., Tarbell, T., Shine, R. A.: *ASP Conference Series*, **397**, 27 (2008)
- Tavabi, E., Koutchmy, S., Ajabshirizadeh, A.: *New Astron.* **16**, 296 (2011)
- Van Doorsselaere, T., Andries, J., Poedts, S.: *Astron. Astrophys.* **471**, 311 (2007)
- Verth, G., Goossens, M., He, J.-S.: *Astrophys. J. Lett.* **733**, 15 (2011)
- Verwichte, E., Nakariakov, V. M., Ofman, L., Deluca, E. E.: *Sol. Phys.* **223**, 77 (2004)
- Vial, J.-C., Ebadi, H., Ajabshirizadeh, A.: *Sol. Phys.* **246**, 327 (2009)
- Wilhelm, K., Curdt, W., Marsch, E., Schühle, U., Lemaire, P., Gabriel, A., Vial, J.-C., Grewing, M., Huber, M. C. E., Jordan, S. D., and 6 coauthors, *Sol. Phys.* **162**, 189 (1995)
- Xia, L.D., Popescu, M.D., Doyle, J.G., Giannikakis, J.: *Astron. Astrophys.* **438**, 1152 (2005)
- Zaqarashvili, T.V., Erdélyi, R.: *Space Sci. Rev.* **149**, 335 (2009)
- Zaqarashvili, T. V., Khodachenko, M. L., Soler, R.: *Astron. Astrophys.* **549**, 113 (2013a)
- Zaqarashvili, T.V., Khutsishvili, E., Kukhianidze, V., Ramishvili, G.: *Astron. Astrophys.* **474**, 627 (2007)
- Zaqarashvili, T.V., Melnik, V.N., Brazhenko, A.I., Panchenko, M., Konovalenko, A.A., Franzuzenko, A.V., Dorovskyy, V.V., Rucker, H.O.: *Astron. Astrophys.* **555**, 55 (2013b)

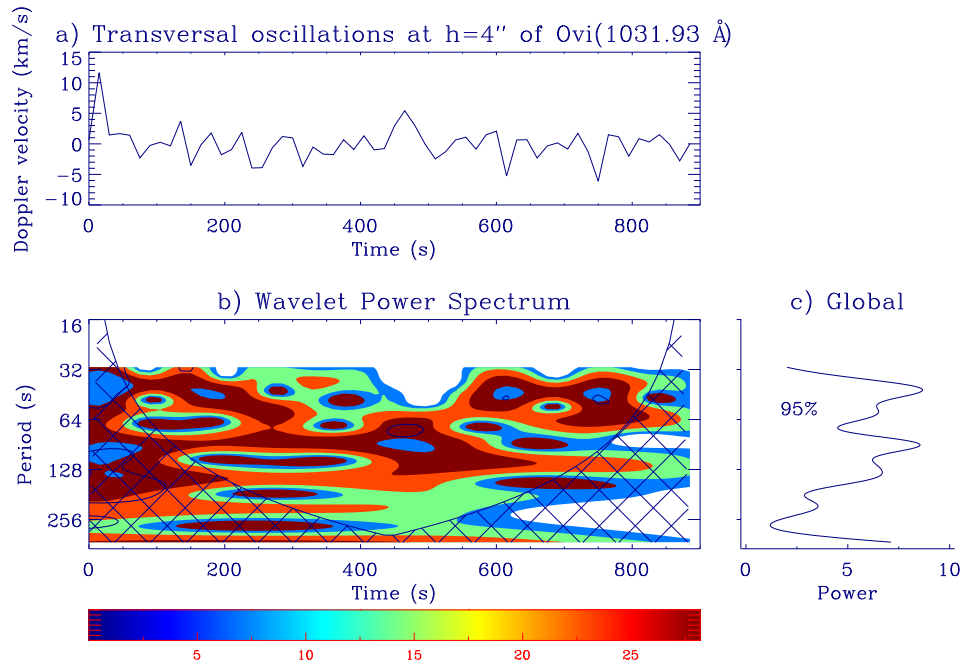


Fig. 4 a. Doppler velocity variations of the studied spicule 4'' above the limb in OVI (1031.93 Å) line. b. The wavelet power spectrum. The contour levels are chosen so that 75%, 50%, 25%, and 5% of the wavelet power is above each level, respectively. The cross-hatched region is the cone of influence, where zero padding has reduced the variance. c. The global wavelet power spectrum.

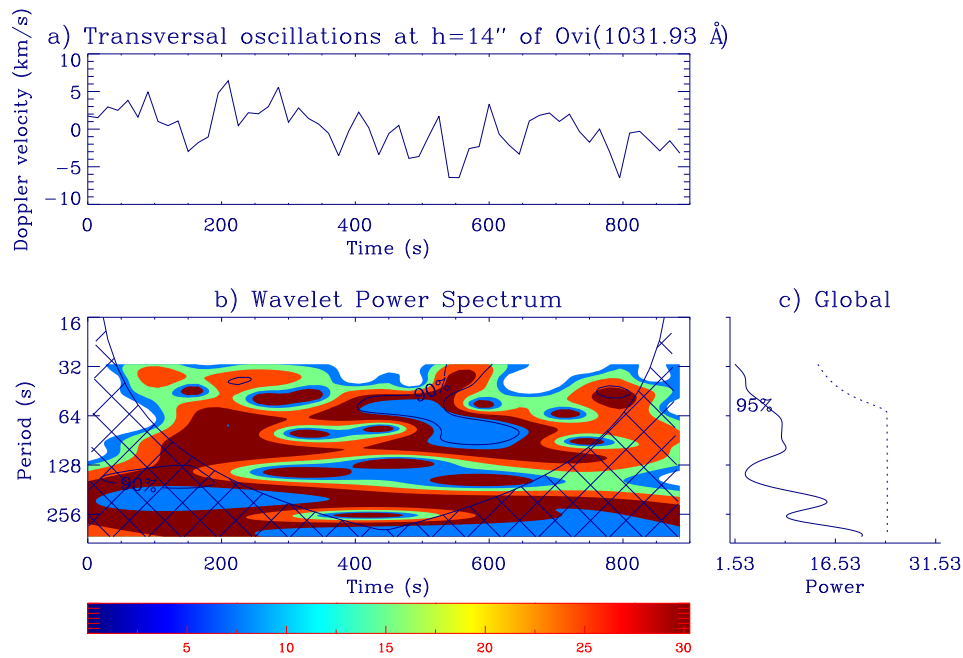


Fig. 5 The same as in Fig. 3 but 14'' above the limb.

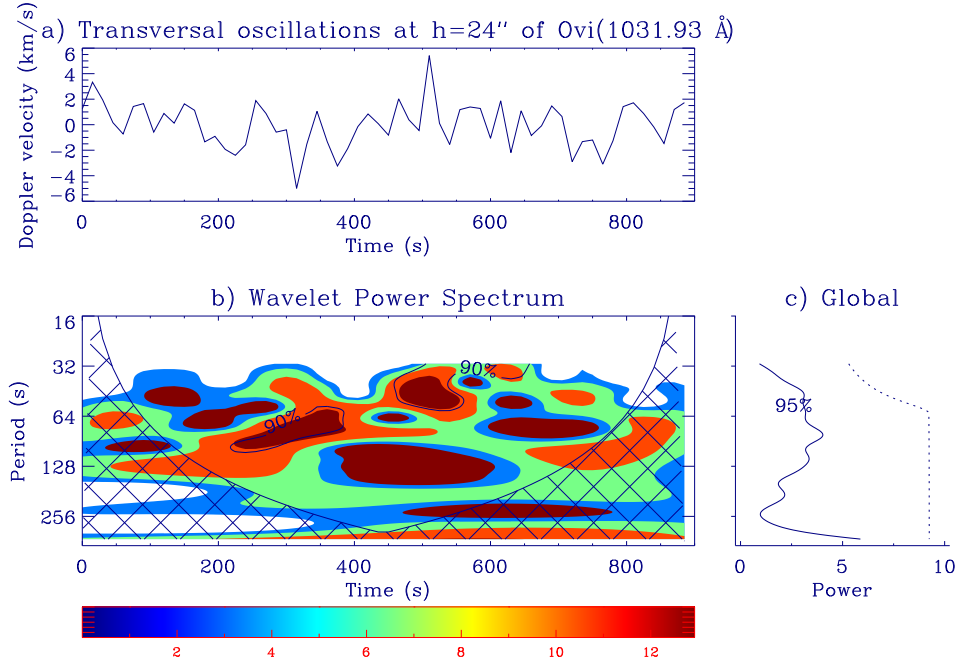


Fig. 6 The same as in Fig. 3 but $24''$ above the limb.

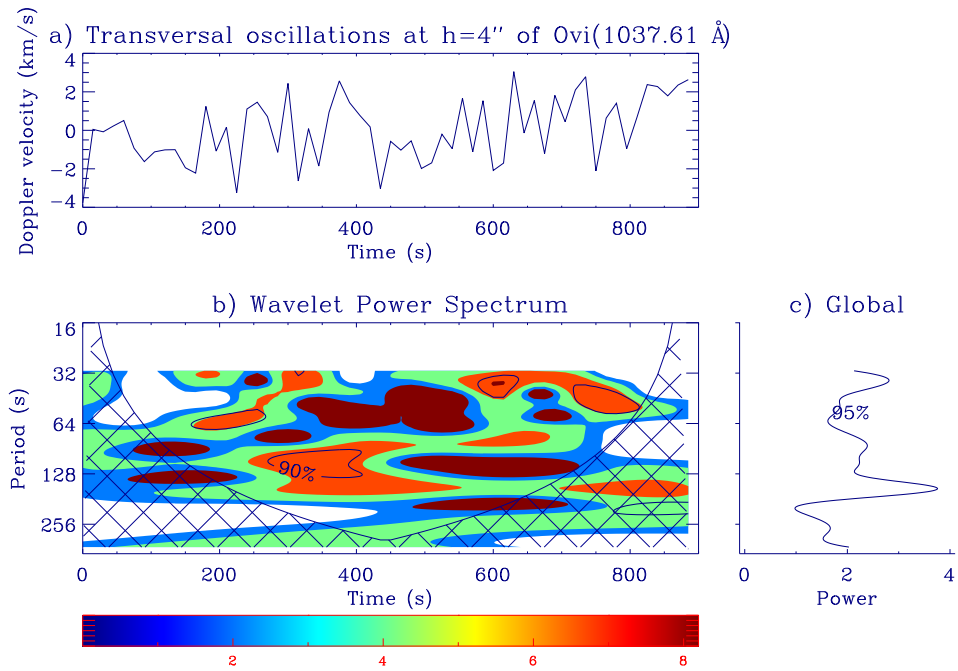


Fig. 7 a. Doppler velocity variations of the studied spicule $4''$ above the limb in OVI (1037.61 Å) line. b. The wavelet power spectrum. The contour levels are chosen so that 75%, 50%, 25%, and 5% of the wavelet power is above each level, respectively. The cross-hatched region is the cone of influence, where zero padding has reduced the variance. c. The global wavelet power spectrum.

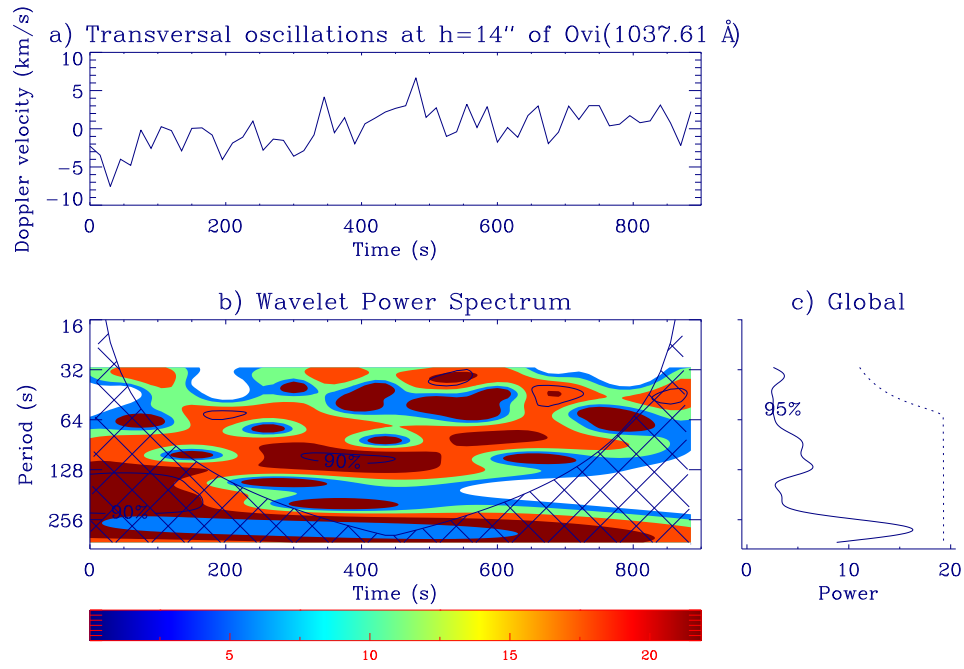


Fig. 8 The same as in Fig. 6 but $14''$ above the limb.

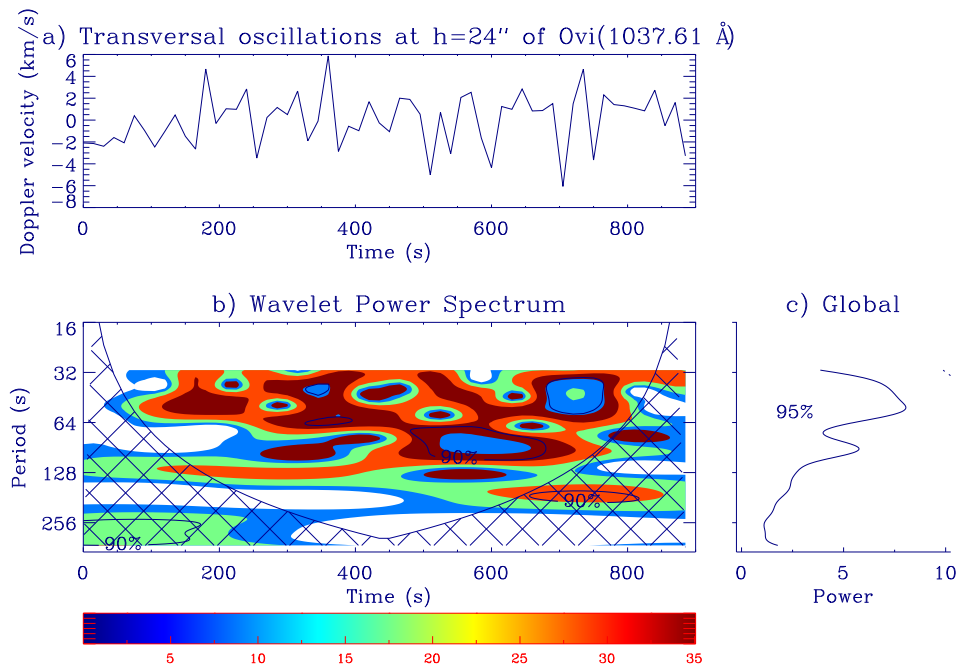


Fig. 9 The same as in Fig. 6 but $24''$ above the limb.